

# UC San Diego

## UC San Diego Previously Published Works

### Title

Freshwater Input and Vertical Mixing in the Canada Basin's Seasonal Halocline: 1975 versus 2006-12

### Permalink

<https://escholarship.org/uc/item/00z3g180>

### Journal

Journal of Physical Oceanography, 52(7)

### ISSN

0022-3670

### Authors

Rosenblum, Erica  
Stroeve, Julienne  
Gille, Sarah T  
[et al.](#)

### Publication Date

2022-07-01

### DOI

10.1175/jpo-d-21-0116.1

Peer reviewed

1 **Freshwater input and vertical mixing in the Canada Basin's seasonal**

2 **halocline:**

3 **1975 versus 2006-2012**

4 Erica Rosenblum\*

5 *Centre for Earth Observation Science, University of Manitoba, Winnipeg, Manitoba, Canada*

6 Julienne Stroeve

7 *Centre for Earth Observation Science, University of Manitoba, Winnipeg, Manitoba, Canada*

8 *Centre for Polar Observation and Modelling, University College London, Earth Sciences,*

9 *London, United Kingdom*

10 *National Snow and Ice Data Center, Cooperative Institute for Research in Environmental*

11 *Sciences, University of Colorado, Boulder, CO, USA*

12 Sarah T. Gille

13 *Scripps Institution of Oceanography, University of California San Diego, La Jolla, California,*

14 *USA*

15 Camille Lique

16 *University of Brest, CNRS, IRD, Ifremer, Laboratoire d'Océanographie Physique et Spatiale*

17 *(LOPS), IUEM, Brest, France*

18  
19  
20  
21  
22  
23  
24  
25  
26  
27  
28  
29  
30  
31  
32  
33

Robert Fajber

*Department of Physics, University of Toronto, Toronto, Ontario, Canada*

L. Bruno Tremblay

*Department of Atmospheric Science, McGill University, Montreal, Quebec, Canada*

Ryan Galley

*Department of Environment and Geography, University of Manitoba, Winnipeg, Manitoba,  
Canada*

Thiago Loureiro

*Toronto, Ontario, Canada*

David G. Barber

*Centre for Earth Observation Science, University of Manitoba, Winnipeg, Manitoba, Canada*

Jennifer V. Lukovich

*Centre for Earth Observation Science, University of Manitoba, Winnipeg, Manitoba, Canada*

*\*Corresponding author address: Erica Rosenblum, Centre for Earth Observation Science, University of Manitoba, Winnipeg, Manitoba, Canada.*

E-mail: [erica.rosenblum@umanitoba.ca](mailto:erica.rosenblum@umanitoba.ca)

## ABSTRACT

34 The Arctic seasonal halocline impacts the exchange of heat, energy, and  
35 nutrients between the surface and the deeper ocean, and it is changing in re-  
36 sponse to Arctic sea ice melt over the past several decades. Here, we assess  
37 seasonal halocline formation in 1975 and 2006-2012 by comparing daily, May  
38 to September, salinity profiles collected in the Canada Basin under sea ice. We  
39 evaluate differences between the two time periods using a one-dimensional  
40 (1D) bulk model to quantify differences in freshwater input and vertical mix-  
41 ing. The 1D metrics indicate that two separate factors contribute similarly  
42 to stronger stratification in 2006-2012 relative to 1975: (1) larger surface  
43 freshwater input and (2) less vertical mixing of that freshwater. The larger  
44 freshwater input is mainly important in August-September, consistent with a  
45 longer melt season in recent years. The reduced vertical mixing is mainly  
46 important from June until mid-August, when similar levels of freshwater in-  
47 put in 1975 and 2006-2012 are mixed over a different depth range, resulting  
48 in different stratification. These results imply that decadal changes to ice-  
49 ocean dynamics, in addition to freshwater input, significantly contribute to  
50 the stronger seasonal stratification in 2006-2012 relative to 1975. These find-  
51 ings highlight the need for near-surface process studies to elucidate the impact  
52 of lateral processes and ice-ocean momentum exchange on vertical mixing.  
53 Moreover, the results may provide insight for improving the representation of  
54 decadal changes to Arctic upper-ocean stratification in climate models that do  
55 not capture decadal changes to vertical mixing.

## 56 **1. Introduction**

57 The surface waters of the Arctic Ocean have changed dramatically over the past several decades  
58 as a result of the diminishing sea ice cover that once shielded much of the ocean from wind and  
59 sunlight across all seasons (Perovich 2011; Stroeve and Notz 2018; Polyakov et al. 2020), and  
60 this has important consequences for the exchange of heat and nutrients between the surface and  
61 deeper ocean (McLaughlin et al. 2011; Carmack et al. 2015; Timmermans and Marshall 2020;  
62 Brown et al. 2020). Changes in Arctic sea ice conditions are generally thought to either strengthen  
63 or weaken the underlying upper-ocean stratification depending on the competing effects of fresh-  
64 water input and of vertical mixing (Peralta-Ferriz and Woodgate 2015; Lique 2015; Nummelin  
65 et al. 2015; Davis et al. 2016). A now warmer atmosphere and ocean delays ice freeze-up, reduces  
66 winter ice growth, and can melt more sea ice each spring and summer, potentially releasing more  
67 fresh, buoyant meltwater to the surface (Stroeve et al. 2014; Carmack et al. 2016) and stabilizing  
68 the upper ocean. Conversely, the wind acts on a now more mobile ice pack (Hakkinen et al. 2008;  
69 Rampal et al. 2009; Spreen et al. 2011; Galley et al. 2013; Kwok et al. 2013; Brown et al. 2020),  
70 potentially generating greater shear that stirs and mixes the underlying ocean, and reducing the  
71 stability of the upper ocean (Lemke and Manley 1984; Polyakov et al. 2020). Increased strati-  
72 fication has been documented in recent decades in many regions of the Arctic, but the evolving  
73 relationship between freshwater input and upper-ocean vertical mixing in response to Arctic sea  
74 ice retreat remains an open question.

75 We examine this question by comparing the seasonal evolution of the upper-ocean salinity below  
76 sea ice during two time periods that are separated by approximately three decades, and that are  
77 associated with distinctly different sea ice conditions. The datasets come from the 1975 Arctic  
78 Ice Dynamics Joint Experiment (AIDJEX) program (Untersteiner et al. 2007) and from the 2004-

79 present Ice-Tethered Profiler (ITP) instrumentation system (Krishfield et al. 2008). Compared to  
80 the 1975 AIDJEX dataset, the ITP dataset is associated with lower sea ice concentration (Fig.  
81 1), has less multi-year sea ice area and volume (Wadhams 2012; Kwok 2018), and is made up  
82 of smaller ice floes (Hutchings and Faber 2018) that are both thinner (Kwok and Rothrock 2009;  
83 Kwok 2018) and less deformed, with shallower ridges (Wadhams 2012; Hutchings and Faber  
84 2018; Kwok 2018).

85 Both the ITP and AIDJEX data were collected in the Canada Basin (Fig. 1), where the upper-  
86 ocean hydrography evolves seasonally in response to changes in sea ice (McPhee and Smith  
87 1976; Morison and Smith 1981; Lemke and Manley 1984; Jackson et al. 2010; Toole et al. 2010;  
88 Peralta-Ferriz and Woodgate 2015), river runoff (Macdonald et al. 1999; Yamamoto-Kawai et al.  
89 2009), and Ekman dynamics in the Beaufort Gyre (Proshutinsky et al. 2009; Carmack et al. 2016;  
90 Meneghello et al. 2018). In the spring and summer, freshwater flux from snow and sea ice melt  
91 causes the surface mixed layer to freshen and shoal, forming a seasonal halocline. The predom-  
92 inant, clockwise atmospheric circulation (Beaufort High) drives convergent Ekman pumping in  
93 the Beaufort Gyre most noticeably in the fall, causing low salinity surface water to converge and  
94 the halocline to deepen within the basin (Reed and Kunkel 1960; Gudkovich 1961; Hunkins and  
95 Whitehead 1992; Proshutinsky et al. 2009; Newton et al. 2006; Jackson et al. 2010; McLaugh-  
96 lin and Carmack 2010; Meneghello et al. 2018). In the winter, sea ice formation results in brine  
97 rejection, which increases the surface water salinity and causes convectively-driven mixed-layer  
98 deepening that erodes the seasonal halocline.

99 Comparisons of single representative profiles from ITP and AIDJEX data that were collected in  
100 roughly the same location indicate a trend toward fresher surface waters, shallower mixed layers,  
101 and a more stably stratified upper ocean (Toole et al. 2010; MCPhee 2012), similar to the com-  
102 parison of AIDJEX and 1997 Surface HEat Budget of the Arctic (SHEBA) data (McPhee et al.

103 1998). June–September and November–May seasonal averages of hydrographic data across the  
104 Arctic during 1979-2012, which did not include ITP or AIDJEX data, confirmed statistically sig-  
105 nificant  $\sim 30$ -year trends toward a more stably stratified upper ocean with shallower and fresher  
106 mixed layers in the Canada Basin (Peralta-Ferriz and Woodgate 2015). Decadal changes to the  
107 surface waters were primarily attributed to increased freshwater input from ice melt, river run-off,  
108 and precipitation. This freshwater has collected toward the center of an intensified anticyclonic  
109 (convergent) Beaufort Gyre (Macdonald et al. 1999; Proshutinsky et al. 2009; Jackson et al. 2010;  
110 McLaughlin and Carmack 2010; Steele et al. 2011; Peralta-Ferriz and Woodgate 2015). However,  
111 the seasonality of the freshwater input, the vertical extent of wind-driven mixing, and upper-ocean  
112 stratification was not addressed in these previous studies.

113 In this study, we compare seasonal processes of the upper ocean by focusing on the evolving time  
114 series from May to September in the 2006-2012 ITP data and 1975 AIDJEX data. This seasonal  
115 analysis differs from previous studies that compared two single profiles (Toole et al. 2010; McPhee  
116 et al. 1998), two 20-day average profiles (McPhee 2012), or used four- and seven-month averages  
117 (Peralta-Ferriz and Woodgate 2015). We interpret the results using a simple one-dimensional bulk  
118 model of seasonal halocline formation that allows for the comparison of the ITP and AIDJEX  
119 data in terms of seasonal freshwater input and vertical mixing. The datasets used for this study  
120 are presented in Section 2, and the one-dimensional model is presented in Section 3. In Section  
121 4, we present results comparing the ITP and AIDJEX hydrographic data in conjunction with the  
122 one-dimensional model metrics. We discuss broad implications of the results for coupled models  
123 and mechanisms that could explain changes in the relationship between freshwater input, vertical  
124 mixing, and stratification during the two time periods in Section 5 and summarize our results in  
125 Section 6.

## 126 **2. Data**

127 This study addresses spring-to-summer halocline formation associated with two distinctly differ-  
128 ent time periods and sea ice regimes. To this end, we use observed May–September near-surface  
129 salinity profiles from the AIDJEX and ITP programs.

130 A major component of the AIDJEX program consisted of four occupied, drifting ice camps  
131 where oceanographic data were collected for approximately one year between May 1975 and  
132 April 1976 (Table 1). Salinity and temperature profiles between depths of 5 m and 750 m were  
133 measured daily at each camp, with a vertical resolution of 1–2 m, using a Plessey model 9040  
134 conductivity, temperature, depth measurement system, resulting in 1279 vertical profiles. See  
135 Maykut and McPhee (1995) for a full description of the data used in this analysis.

136 The ITP instrument system records temperature and salinity profiles with a vertical resolution of  
137 25 cm throughout the Arctic. The system consists of a series of surface buoys, frozen into drifting  
138 ice floes, connected to 800-m-long wires. CTD profilers move up and down the wires collecting  
139 data approximately 2-3 times per day. We use quality-controlled data, identified as level 3 in the  
140 ITP data archives, which have 1 m vertical resolution and were available for 2004-2012 at the  
141 time of the analysis. We examine all available level-3 processed data within the Canada Basin,  
142 which we define as the region bounded by 72°N, 80°N, 130°W, and 155°W (similar to the region  
143 defined by Peralta-Ferriz and Woodgate (2015); dashed lines, Fig. 1). Further, we select only ITPs  
144 that have data starting in May of a given year, similar to the data available from the AIDJEX ice  
145 camps. Lastly, profiles were removed if the shallowest observed value was deeper than 10 meters  
146 (following Jackson et al. 2010), which helps to account for the fact that ITPs often start sampling  
147 too deep to accurately measure the summer mixed layer.



148 In total, 517 AIDJEX profiles collected in 1975 from 4 ice camps and 2892 ITP profiles col-  
149 lected between 2006-2012 from 12 different ITPs satisfied these criteria (Table 1), with average  
150 shallowest measurements of  $\sim 6$  m and  $\sim 7$  m, respectively. All profiles were linearly interpolated  
151 onto a common 1-m vertical grid. Ice thickness measurements are not available for all ITP pro-  
152 files or AIDJEX ice camps. For both datasets, we therefore assume an ice–ocean interface at 3 m,  
153 a climatological multi-year sea ice thickness in the Canada Basin (Perovich and Richter-Menge  
154 2015), and keep the salinity and temperature constant from the shallowest measurements of each  
155 profile to  $z = -3$  m, with the  $z$ -axis defined as positive up. We discuss the sensitivity of our results  
156 to missing near-surface data in Section 5.

157 To estimate the freshwater input from sea ice melt, we also examine 1979-2018 sea ice volume  
158 estimates provided by the Pan-arctic Ice Ocean Modeling and Assimilation System (PIOMAS,  
159 Schweiger et al. 2011). The PIOMAS sea ice volume was regridded to the 25 km Equal-Area  
160 Scalable Earth (EASE) grid and averaged over the Canada Basin (bounded by  $72^\circ\text{N}$ ,  $80^\circ\text{N}$ ,  $130^\circ\text{W}$ ,  
161 and  $155^\circ\text{W}$ , as in the hydrographic data).

162 To qualitatively compare the sea ice conditions associated with the AIDJEX and ITP datasets,  
163 we examine 1975 and 2006-2012 sea ice concentrations. Daily 2006-2012 sea ice concentra-  
164 tion observations are provided by Passive Microwave satellite data, Version 1 (Cavalieri et al.  
165 1996), which combines data from the Defense Meteorological Satellite Program Special Sen-  
166 sor Microwave/Imager (DMSP SSM/I, 2006-2007) and the Special Sensor Microwave Imager/  
167 Sounder (SSMIS, 2007-2012). Sea ice concentration data are co-located to each ITP observation.  
168 We note that low sea ice concentration from the passive microwave data can imply either low ice  
169 concentration or surface melt ponds (e.g., Kern et al. 2016). Since the AIDJEX data were collected  
170 in 1975, before the satellite data were available, we use the Canadian Ice Service digital archive  
171 (CISDA) chart data for the western Arctic region to determine the temporal evolution of sea ice

172 concentration during that year in the Canada basin region (Tivy et al. 2011). Gridded datasets for  
173 each CISDA chart in June-September 1975 were analyzed to provide a weekly regional mean sea  
174 ice concentration.

### 175 **3. One-Dimensional Framework**

176 One-dimensional (1D) ice-ocean bulk models are used to provide a framework for interpreting  
177 observed seasonal mixed-layer evolution (Morison and Smith 1981; Lemke and Manley 1984;  
178 Lemke 1987; Toole et al. 2010; Petty et al. 2013; Tsamados et al. 2015; Peralta-Ferriz and  
179 Woodgate 2015; Randelhoff et al. 2017). Here, we model seasonal halocline formation starting  
180 from a homogeneous winter mixed layer in an idealized system (Fig. 2), building on conceptual  
181 models used to estimate freshwater input, vertical mixing, and upper-ocean stratification from hy-  
182 drographic data in previous studies (Lemke and Manley 1984; Peralta-Ferriz and Woodgate 2015;  
183 Randelhoff et al. 2017). The resulting framework provides a suite of diagnostic, upper-ocean pa-  
184 rameters to examine the vertical salt budget and its impact on the stratification using the observed  
185 seasonal evolution of vertical salinity profiles. This idealized model omits a range of processes, in-  
186 cluding (1) temperature effects on density, which have a less than 1% impact of the surface density  
187 in the ITP data (not shown), (2) brine-rejection driven mixing from intermittent freezing, which  
188 cannot be resolved from daily observations; (3) tidal currents, which are only expected to impact  
189 shelf waters (i.e. shallower than in the Canada Basin), (4) double-diffusion, which mainly impacts  
190 the 200-300 m depth range in this region (Timmermans et al. 2008), and a range of processes  
191 associated with horizontal advection; the impact of this will be considered in Sections 4-5.

192 *a. Model Equations*

193 We consider a closed, 1D ice-ocean system with an ocean of depth  $L$  that only evolves in re-  
 194 sponse to thermodynamic spring-summer sea ice melt and vertical mixing with the following ini-  
 195 tial conditions ( $t = t_0$ ): a well-mixed ocean, with vertically uniform salinity ( $S_0$ ) and potential  
 196 density ( $\rho_0$ ), and sea ice with constant salinity ( $S_{ice}$ ) and density ( $\rho_{ice}$ ).

197 If melt water is vertically mixed to some depth,  $Z_{fw}$ , then the salinity and density below this  
 198 depth remains fixed at  $S_0$  and  $\rho_0$  (i.e.,  $S(z) = S_0$  and  $\rho(z) = \rho_0$  for  $z \leq Z_{fw}$ , where  $z$  and  $Z_{fw}$  are  
 199 both negative). The conservation of salt and mass for time  $t > t_0$  can then be written as:

$$\int_{Z_{fw}(t)}^{Z_{ice}} \rho(t, z) S(t, z) \cdot dz - \rho_0 S_0 (Z_{ice} - Z_{fw}(t)) = \rho_{ice} S_{ice} h_{melt}(t) \quad (1)$$

$$\int_{Z_{fw}(t)}^{Z_{ice}} \rho(t, z) \cdot dz - \rho_0 (Z_{ice} - Z_{fw}(t)) = \rho_{ice} h_{melt}(t), \quad (2)$$

200 where  $t$  is a seasonally evolving time variable,  $Z_{ice}$  is the ice draft,  $h_{melt}$  is the change in sea ice  
 201 thickness from melt,  $\rho(t, z)$  and  $S(t, z)$  are the ocean potential density and salinity, respectively.  
 202 The above expressions, therefore, represent the change in mass and salt in the ocean (left-hand  
 203 side) in response to sea ice melt (right-hand side). These equations can be algebraically combined  
 204 to estimate the sea ice melt necessary to explain the transition from the initial, well-mixed ocean  
 205 ( $S_0, \rho_0$ ) to the subsequent ocean profile that includes vertically mixed meltwater ( $S(t, z), \rho(t, z)$ ) at  
 206 any time  $t > t_0$ :

$$h_{melt}(t) = \int_{Z_{fw}(t)}^{Z_{ice}} \frac{\rho(t, z)(S(t, z) - S_0)}{\rho_{ice}(S_{ice} - S_0)} \cdot dz, \quad (3)$$

207 where  $h_{melt}$  represents a time-evolving integral measure of seawater dilution by cumulative surface  
 208 freshwater input from sea ice melt. This approach is similar to an approach used in previous  
 209 studies that estimated sea ice melt from mixed-layer salinity evolution (Lemke and Manley 1984;  
 210 Peralta-Ferriz and Woodgate 2015), but here the depth range is set by  $Z_{fw}$  and  $Z_{ice}$  rather than a  
 211 mixed-layer depth criterion. That is, we estimate the freshwater input from sea ice melt over a

212 well-defined volume, which avoids errors that can arise when using an arbitrary reference salinity  
 213 (Schauer and Losch 2019; Rosenblum et al. 2021).

214 The term  $h_{melt}$  is linearly related to the vertically integrated change in salinity relative to  $S_0$ :

$$\Phi(t) = \int_{Z_{fw}(t)}^{Z_{ice}} S_0 - S(t, z) \cdot dz, \quad (4)$$

215 which also provides a bulk estimate of the cumulative amount of freshwater input at any time  
 216  $t > t_0$ . We note that  $\Phi$  is closely related to the “salt deficit” or “buoyancy deficit” as defined by  
 217 Martinson (1990), Martinson and Iannuzzi (1998), and Randelhoff et al. (2017).

218 Different salinity profiles are possible in response to the same amount of ice melt, depending on  
 219 how the melt water is vertically spread or mixed through the water column (Fig. 2). For example,  
 220 if the melt water were concentrated close to the surface (less vertical mixing, shallow  $Z_{fw}$ ), this  
 221 would result in more surface freshening and a more stably stratified water column (Fig. 2; left  
 222 side). Alternatively, if the melt water were spread over a larger depth range (more vertical mixing,  
 223 deep  $Z_{fw}$ ), this would result in less surface freshening and a less stably stratified water column  
 224 (Fig. 2; right side).

225 To quantify this effect, we will consider two bulk metrics of stratification. First, we define the  
 226 surface freshening at any time  $t > t_0$  as the surface salinity anomaly relative to the initial condition:

$$\delta S_{surf}(t) = S(t, Z_{ice}) - S_0. \quad (5)$$

227 Second, we define the stratification that occurs in response to sea ice melt at any time  $t > t_0$  as the  
 228 vertical derivative of salinity averaged over depth  $Z_{fw}$ :

$$S_z(t) = \frac{1}{Z_{fw}(t) - Z_{ice}} \int_{Z_{fw}(t)}^{Z_{ice}} \frac{dS(t, z)}{dz} dz. \quad (6)$$

229 *b. Separating freshwater input and vertical mixing*

230 We seek representations of  $\delta S_{surf}$  and  $S_z$  to directly compare the 1975 AIDJEX data and 2006-  
231 2012 ITP data in terms of changes to (1) the seasonal freshwater input and (2) vertical mixing.

232 That is, for any time  $t > t_0$ , we seek:

$$\Delta(\delta S_{surf}(t)) = f(\Delta\Phi(t), \Delta D(t)) \quad (7)$$

$$\Delta S_z(t) = f(\Delta\Phi(t), \Delta D(t)). \quad (8)$$

233  $\Delta$  indicates the difference between ITP and AIDJEX data:

$$\Delta X = X_{ITP} - X_{AJX}, \quad (9)$$

234 where *ITP* indicates that the value is derived from ITP data and *AJX* indicates that the value is  
235 derived from AIDJEX data.

236  $D$  is a bulk indicator of the vertical mixing, where we define larger and smaller mixing as mixing  
237 that leads to a deeper or shallower seasonal halocline. We choose the equivalent mixed-layer depth,  
238 an integral quantity that is closely related to the vertical extent of wind-driven mixing (similar to  
239 (Randelhoff et al. 2017)):

$$D(t) = \frac{\Phi(t)}{\delta S_{surf}(t)}, \quad (10)$$

240 where  $D + Z_{ice}$  indicates the depth of the halocline if the meltwater were completely mixed (i.e., if  
241 the salinity were homogenized), implying that the salinity profile would have a 2-layer form and  
242 that  $D + Z_{ice} = Z_{fw}$ :

$$S_{bulk}(t, z) = \begin{cases} S_0 + \Phi(t)/D(t) & D(t) + Z_{ice} \leq z \leq Z_{ice} \\ S_0 & z < D(t) + Z_{ice} \end{cases} \quad (11)$$

243 (see Fig. 2 for an illustration of this 2-layer profile).

244 The surface freshening ( $\delta S_{surf}$ ) and stratification ( $S_z$ ) associated with this 2-layer system for any  
 245 time  $t \geq t_0$  is:

$$\delta S_{surf}(t) = \frac{\Phi(t)}{D(t)} \quad \text{and} \quad S_z(t) = \frac{\Phi(t)}{D(t)^2}, \quad (12)$$

246 respectively, following equations (5), (6), and (11).  $\delta S_{surf}$ , therefore, indicates the salt content  
 247 changes within the mixed layer  $D$ .

248 Two factors determine  $\delta S_{surf}$  and  $S_z$ : (1) the amount of freshwater input (related to  $\Phi$  and  $h_{melt}$ )  
 249 and (2) the concentration or dilution of that freshwater toward or away from the surface by vertical  
 250 mixing (related to  $D$ ). We can, therefore, estimate how each factor contributes to  $\Delta(\delta S_{surf})$  and  
 251  $\Delta S_z$  (as in eqs. 7-8) by writing  $\delta S_{surf}$  and  $S_z$  derived from 2006-2012 ITP data in terms of the  
 252 changes relative to the 1975 AIDJEX data:

$$\delta S_{surf,ITP}(t) = \frac{\Phi_{AJX}(t) + \Delta\Phi(t)}{D_{AJX}(t) + \Delta D(t)}, \quad (13)$$

$$S_{z,ITP}(t) = \frac{\Phi_{AJX}(t) + \Delta\Phi(t)}{(D_{AJX}(t) + \Delta D(t))^2}. \quad (14)$$

253 The difference between  $\delta S_{surf}$  in 1975 and 2006-2012 ( $\Delta(\delta S_{surf})$ ) can then be re-written alge-  
 254 braically to isolate the relative contributions of  $\Delta\Phi$  and  $\Delta D$  on  $\Delta(\delta S_{surf})$ :

$$\Delta(\delta S_{surf}(t)) = \underbrace{\frac{\Delta\Phi(t)}{D_{AJX}(t)}}_{\text{changes to freshwater input}} - \underbrace{\frac{\Phi_{AJX}(t)\Delta D(t)}{D_{AJX}(t)D_{ITP}(t)}}_{\text{changes to vertical mixing}} - \underbrace{\frac{\Delta\Phi(t)\Delta D(t)}{D_{AJX}(t)D_{ITP}(t)}}_{\text{correlated term}}. \quad (15)$$

255 Similarly, the difference between  $S_z$  in 1975 and 2006-2012 ( $\Delta S_z$ ) can be written as:

$$\Delta S_z(t) = \underbrace{\frac{\Delta\Phi(t)}{D_{AJX}(t)^2}}_{\text{changes to freshwater input}} - \underbrace{\Phi_{AJX}(t)\Delta D(t)\frac{D_{AJX}(t) + D_{ITP}(t)}{D_{AJX}^2(t)D_{ITP}^2(t)}}_{\text{changes to vertical mixing}} - \underbrace{\Delta\Phi(t)\Delta D(t)\frac{D_{AJX}(t) + D_{ITP}(t)}{D_{AJX}^2(t)D_{ITP}^2(t)}}_{\text{correlated term}}. \quad (16)$$

256 (See Supporting Information for full derivation.)

257 The three terms on the right-hand sides of (15) and (16) are estimates of the decadal changes  
 258 to the stratification associated with (1) changes related to only freshening (freshwater input;  $\Delta\Phi$ ,

259  $\Delta h_{melt}$ ), holding the vertical mixing to AIDJEX values ( $D_{AJX}$ ); (2) changes related to only mixed-  
260 layer shoaling (vertical mixing;  $\Delta D$ ), holding the amount of freshwater input equal to AIDJEX  
261 values ( $\Phi_{AJX}$ ); and (3) the contribution from the correlation between  $\Delta\Phi$  and  $\Delta D$ .

## 262 4. Results

263 The observations indicate that the surface is  $\sim 2$ -4 g/kg fresher in 2006-2012 relative to 1975, yet  
264 both time periods have a similar seasonal evolution (Fig. 3). At the beginning of May, both datasets  
265 indicate mixed layers that are relatively deep (thick black lines, Fig. 3a). As spring progresses, the  
266 surface freshens and the seasonal halocline forms (dashed black lines, Fig. 3a,b). Toward the end  
267 of summer, sea ice forms, the surface becomes progressively saltier, and the mixed layer deepens,  
268 eroding the seasonal halocline (compare dashed and thick black lines, Fig. 3b). Compared to  
269 1975, 2006-2012 appears to have more seasonal freshwater stored closer to the surface, resulting  
270 in more seasonal surface freshening and a more stably stratified upper ocean for a longer time  
271 period. Qualitatively, this is consistent with the previous studies described in Section 1.

272 To compare the seasonal evolution of the upper ocean during 1975 and 2006-2012 using the 1D  
273 framework, we set  $S_0$  equal to the May-average surface salinity ( $S(Z_{ice})$ ) measured by the same  
274 ITP or AIDJEX ice camp during the same year. That is, we examine the seasonal freshwater  
275 input ( $\Phi$ ,  $h_{melt}$ ), vertical mixing ( $Z_{fw}$ ,  $D$ ), and the surface freshening ( $\delta S_{surf}$ ) relative to the May  
276 average, which marks the beginning of the melt season measured by a given ITP or AIDJEX ice  
277 camp. We present results based on alternative values of  $S_0$  in the Supporting Information. All  
278 other constants are given in Table 2.

279 Figure 4 shows an example of how various quantities presented in Section 3 are computed for  
280 a single profile using observations from one AIDJEX ice camp (Fig. 4; left side) and one ITP  
281 (Fig. 4; right side). The freshwater input, indicated by  $h_{melt}$  and  $\Phi$ , reflects any process that drives

282 changes to the integrated upper-ocean salinity, including sea ice melt, river runoff, precipitation,  
283 or advection, although previous studies have demonstrated that the majority of the seasonal fresh-  
284 water input during the melt season is derived from sea ice melt (e.g., Lemke and Manley 1984;  
285 Peralta-Ferriz and Woodgate 2015). Vertical mixing, indicated by  $Z_{fw}$  and  $D$ , reflects any process  
286 that vertically spreads or distributes that freshwater, including wind-driven mixing, and possibly  
287 brine-rejection from intermittent freezing, double-diffusion, or tidal currents.

### 288 *a. Validation*

289 To test the validity of our approach, we compare the cumulative seasonal freshwater input in  
290 terms of the equivalent ice melt ( $h_{melt}$ ), derived from hydrographic data, to the effective ice thick-  
291 ness change relative to May of each year between 1979-2018 using PIOMAS. We compute  $h_{melt}$   
292 associated with each profile in 1975 and 2006-2012. The seasonal evolution of  $h_{melt}$  and the  
293 monthly ice thickness relative to May are shown in Figure 5. Both estimates indicate cumulative  
294 sea ice melt through August. In 1975,  $h_{melt}$  begins to decrease in early September in response to  
295 sea ice formation and entrainment. In 2006-2012,  $h_{melt}$  continues to moderately increase through  
296 September in response to a later freeze up (Fig. 5a). We find similar results using different defini-  
297 tions of  $S_0$  (Fig. S2).

298 We find good agreement between the PIOMAS seasonal ice thickness changes and the esti-  
299 mated seasonal freshwater input, represented as equivalent meters of ice melt using oceanographic  
300 observations during summer, consistent with previous studies. By the end of August, we find  
301  $h_{melt} \sim 0.5-1$  m in 1975 and  $h_{melt} \sim 1-2$  m in 2006-2012, consistent with estimated sea ice melt  
302 during similar time periods using hydrographic data (Lemke and Manley 1984; Peralta-Ferriz  
303 and Woodgate 2015) and ice mass balance buoys (e.g., Perovich and Richter-Menge 2015). The  
304 consistency of these findings provides indirect evidence that  $h_{melt}$  is a reasonable estimate of the



305 seasonal freshwater input. We note that in June, some data points indicate a negative  $h_{melt}$ . For the  
306 remainder of the analysis, we only consider profiles with positive values of  $h_{melt}$ .

307 Using each observed profile, we compare the stratification ( $S_z$ ; eq. 6) to the associated 2-layer  
308 estimate (eq. 12). The seasonal evolution of each of these values in the 1975 AIDJEX and 2006-  
309 2012 ITP datasets is shown in Figure 6. We find a clear agreement between the observations and  
310 the 2-layer estimates. First, both values indicate that the seasonal halocline forms in late June  
311 of 1975 and 2006-2012, but is more stably stratified for a longer period of time in 2006-2012.  
312 Second, both values are up to five times larger in 2006-2012 relative to 1975. Toward the end of  
313 the melt season, more freshwater is stored below the mixed layer, causing the 2-layer formalism to  
314 overestimate  $S_z$ . Despite these differences, overall, we find that the 2-layer simplification captures  
315 the majority of the key features necessary to explain the differences between the upper-ocean  
316 seasonal evolution in 1975 and 2006-2012.

317 The equivalent mixed-layer depth ( $D$ ) and the associated surface freshening ( $\delta S_{surf}$ ) in 1975  
318 and 2006-2012 are shown in Figure 7. These metrics indicate a number of differences between  
319 the ITP and AIDJEX datasets that are consistent with previously documented decadal trends in  
320 the Canada Basin. Specifically, Peralta-Ferriz and Woodgate (2015) found statistically significant  
321 trends of mixed-layer freshening (0.11 psu/yr) and mixed-layer shoaling (0.33 m/yr) during June–  
322 September in regions of the Canada Basin with high sea ice concentration (>15%). These rates  
323 of change would imply an average change of 3.7 psu and 11.2 m over 34 years, similar to the  
324 3.1 g/kg and 14.5 m difference in the surface salinity ( $\delta S_{surf} + S_0$ ) and the equivalent mixed-layer  
325 depth ( $D$ ) between the 1975 AIDJEX data and the 2006-2012 ITP data over the same months.  
326 Overall, these findings suggest that a comparison of the ITP and AIDJEX datasets, in conjunction  
327 with the one-dimensional framework presented in Section 3, yields results that are consistent with  
328 Peralta-Ferriz and Woodgate (2015) using seasonal averages.

329 *b. 1975 vs 2006-2012*

330 The relationship between 1D bulk estimates of freshwater input from ice melt and other fresh-  
331 water sources ( $h_{melt}$ ; eq. 3), vertical mixing ( $D$ ; eq. 10), and upper-ocean stratification ( $\delta S_{surf}$ ,  $S_z$ ;  
332 eq. 12) is shown in Figure 8, using every June-September salinity profile in 1975 and 2006-2012.  
333 During each time period, we find that the parameters exhibit relationships that are qualitatively  
334 consistent with a 1D system: Surface fluxes that result in a more buoyant surface layer cause  
335 a more stable stratification that inhibits vertical mixing (Turner 1967; Kraus and Turner 1967;  
336 Lemke and Manley 1984; Lemke 1987). That is, profiles with more freshwater input (larger  $h_{melt}$ )  
337 are associated with less vertical mixing (smaller  $|D|$ , where  $|\cdot|$  indicates the absolute value) and a  
338 more stably stratified upper ocean (large  $|\delta S_{surf}|$ ,  $S_z$ ).

339 Considering differences between 1975 and 2006-2012, we find that there are more profiles in  
340 2006-2012 with large values of  $h_{melt}$  and hence small values of  $|D|$  and large values of  $|\delta S_{surf}|$   
341 and  $S_z$ , as in a 1D system. However, we also consistently find profiles with the same amount of  
342 freshwater ( $h_{melt}$ ) in both time periods but with the freshwater concentrated closer to the surface  
343 (smaller  $|D|$ ) in 2006-2012 relative to 1975 (Fig. 8a). These differences in  $|D|$  are also associated  
344 with a more stable stratification (large  $|\delta S_{surf}|$ ,  $S_z$ ; Fig. 8b-c). That is, there are two separate  
345 factors causing the more stable stratification in 2006-2012 relative to 1975: (1) more freshwater  
346 input (larger  $h_{melt}$ ), which mainly occurs in August and September, and (2) less vertical mixing  
347 (smaller  $|D|$ ), which mainly occurs in June and July (Fig. 8; compare top and bottom panels).

348 We find similar results when examining the relationship between  $\Delta(\delta S_{surf})$ ,  $\Delta S_z$ , and  $\Delta h_{melt}$   
349 during each 5-day period (Fig. 9); 5-day periods with similar levels of freshwater input in 1975  
350 and 2006-2012 ( $\Delta h_{melt} \sim 0$ ) have different stratification ( $|\Delta(\delta S_{surf})| > 0$ ,  $\Delta S_z > 0$ ) from June until

351 mid-August. The largest difference between the two time periods occurs from mid-August through  
352 September, coinciding with the largest values of  $\Delta h_{melt}$ .

353 We can use the 1D framework (Section 3b) to estimate the relative importance of each of these  
354 factors in setting the more stable stratification in 2006-2012 relative to 1975. Figure 10b-c shows  
355 the 5-day average bulk estimates of the upper-ocean stratification ( $\delta S_{surf}$ ,  $S_z$ ) in 1975 (blue line)  
356 and 2006-2012 (red line). For each 5-day period, we compute the difference between 1975 and  
357 2006-2012 ( $\Delta(\delta S_{surf}), \Delta S_z$ ) in terms of (1) the larger freshwater input alone (yellow region;  $\propto$   
358  $\Delta h_{melt}$ ,  $\Delta\Phi$ ), (2) the concentration of the freshwater closer to the surface alone (purple region;  
359  $\propto \Delta D$ ), and (3) the contribution from the correlation between the two factors (green region;  $\propto$   
360  $\Delta h_{melt}\Delta D$ ,  $\Delta\Phi\Delta D$ ) using equations (15) and (16). The yellow region provides a rough estimate  
361 of the change in stratification that would occur if the relatively large amount of freshwater input  
362 indicated by 2006-2012 ITP data is stored within the relatively deep mixed layer measured by  
363 1975 AIDJEX data (i.e., if  $\Delta D = 0$  in eqs. (15) and (16)). Similarly, the purple region provides  
364 a rough estimate of the change in stratification that would occur if the relatively small amount  
365 of freshwater input indicated by 1975 AIDJEX data is stored within the relatively shallow mixed  
366 layer measured by 2006-2012 ITP data (i.e., if  $\Delta\Phi = 0$  in eqs. (15),(16)).

367 Overall, the changes to the vertical mixing ( $\Delta D$ ), the freshwater input ( $\Delta\Phi$ ), and the contribution  
368 from the correlation between the two terms ( $\Delta\Phi\Delta D$ ) have similar roles in explaining the larger  
369 magnitudes of  $|\Delta(\delta S_{surf})|$  and  $S_z$  in 2006-2012 relative to 1975. This implies that the concentration  
370 of freshwater closer to the surface in recent years has a similar impact on upper-ocean stratification  
371 to that caused by a larger amount of seasonal freshwater input. The seasonality of the two factors  
372 confirms our findings from Figure 9: The concentration of freshwater closer to the surface (purple  
373 region) is mainly important in June–August, while the larger amount of freshwater input and the  
374 correlated term (yellow and green regions) are mainly important in August–September. This result

375 is also consistent with the the largest differences in  $h_{melt}$  between the two time periods occurring  
376 toward the end of the melt season (Fig. 10a).

## 377 **5. Discussion**

378 Coupled ice-ocean models and global climate models are used extensively to understand current  
379 climate change and to predict future changes, but tend to simulate an upper-ocean stratification in  
380 the Canada Basin that is weaker than observed (Holloway et al. 2007; Ilicak et al. 2016; Nguyen  
381 et al. 2009; Zhang and Steele 2007; Jin et al. 2012; Barthélemy et al. 2015; Sidorenko et al. 2018;  
382 Rosenblum et al. 2021). In a climate model,  $\Phi$  is directly related to the freshwater flux at the  
383 surface due to sea ice melt, river run-off, and precipitation, while  $D$  is closely related to simulated  
384 ocean mixed-layer dynamics (Rosenblum et al. 2021). In Figure 10, the yellow region provides  
385 a rough estimate of the more stable stratification that would occur in a model that accurately  
386 simulated decadal changes to freshwater fluxes with unchanged mixed-layer dynamics. The purple  
387 region provides a rough estimate of the more stable stratification that would occur in a model  
388 that accurately simulated decadal changes to mixed-layer dynamics without simulating changes to  
389 freshwater fluxes. Climate models that do not simulate the decadal trend toward a shallower mixed  
390 layer in the Canada Basin (Rosenblum et al. 2021), therefore, do not include the contributions  
391 toward a more stratified upper-ocean that are quantified by the purple and green regions of Figure  
392 10.

393 What mechanisms caused shallower mixed layers and stronger stratification in 2006-2012 in re-  
394 sponse to the same amount of freshwater input as in 1975 (associated with the purple regions of  
395 Figure 10)? One possibility is that lateral processes are more prominent under the more mobile  
396 ice cover in recent years and cause complicated relationships between freshwater input, vertical  
397 mixing, and stratification (Randelhoff et al. 2017; Meneghello et al. 2021) or establish fronts that

398 act to limit the effects of wind-driven vertical mixing via submesoscale instabilities (Timmermans  
399 and Winsor 2013). A second possibility is that wind-driven momentum transfer below sea ice has  
400 decreased in response to changing sea ice conditions, which can occur in regions that transitioned  
401 from multi-year to first-year ice. Specifically, modeling studies suggest that the wind-driven mo-  
402 mentum transfer can sometimes decrease in response to the loss of ice keels and reduced sea ice  
403 roughness rather than increase in response to enhanced sea ice motion (McPhee 2012; Martin et al.  
404 2014, 2016; Tsamados et al. 2014). A third possibility is that the shallower and more stably strati-  
405 fied winter halocline in 2006-2012 inhibited mixed-layer deepening to the levels seen in 1975 (Fig.  
406 3; Toole et al. 2010; Peralta-Ferriz and Woodgate 2015). Each of these mechanisms would create  
407 a positive feedback scenario in which the same amount of melt water is concentrated closer to the  
408 surface toward the beginning of spring, setting up a more stable seasonal halocline that further  
409 inhibits vertical mixing of meltwater and further stabilizes the seasonal halocline.

410 Another possibility is that changes to the sea ice conditions impact melt-pond drainage, which  
411 is associated with halocline formation in early summer (Gallaher et al. 2016). Unfortunately,  
412 both the ITPs and AIDJEX measurements begin at an average of  $\sim 6-7$  m depth and, therefore,  
413 do not capture important variations to the freshwater content near the surface. This surface data  
414 gap can cause mixed-layer depths to be biased too deep (Toole et al. 2010), can cause the timing  
415 of the mixed-layer shoaling to be biased several weeks too late (Gallaher et al. 2017), and can  
416 cause uncertainties in the seasonal freshwater storage. Considering results from Proshutinsky  
417 et al. (2009), we estimate that this error could cause  $h_{melt}$  to be underestimated by approximately  
418 0.2 m during the summer months (see SI for details). More uncertainties arise because we lack  
419 measurements of the sea ice draft ( $Z_{ice}$ ) for the vertical bounds of our calculations. For example,  
420 we find that  $\pm 1$  m changes to  $Z_{ice}$  result in approximately  $\pm 0.1$  m of equivalent ice melt by the  
421 end of the melt season.

422 Overall, the cause of the shallower vertical mixing in recent years remains an open question but  
423 one that may be essential for accurately simulating decadal changes to upper-ocean stratification  
424 in climate models (Rosenblum et al. 2021). A clear answer to this question will require shallow,  
425 near-ice hydrographic or sea ice mass balance measurements in tandem with models to disentangle  
426 the sensitivity of vertical mixing to lateral processes, ice-ocean momentum exchange, and pre-melt  
427 conditions.

## 428 **6. Summary**

429 The rapid and continuing change of summer sea ice cover in the Canada Basin has led to a  
430 fresher and more stratified upper ocean that has been primarily attributed to more freshwater input  
431 from sea ice melt, river-run off, and Ekman convergence of fresh surface waters within the Beau-  
432 fort Gyre (e.g., McPhee et al. 1998; Macdonald et al. 1999; Yamamoto-Kawai et al. 2009; Jackson  
433 et al. 2010; McLaughlin and Carmack 2010; Steele et al. 2011; Peralta-Ferriz and Woodgate 2015;  
434 Carmack et al. 2015). The results presented here indicate that decadal changes to ice-ocean dy-  
435 namics have a similar impact on the changing seasonal halocline as changes to the freshwater  
436 input.

437 We compared the seasonal evolution of the upper ocean salinity below sea ice in 1975 and 2006-  
438 2012, using data collected from the AIDJEX ice camps and ITPs (Fig. 1; Section 2). We interpret  
439 differences between the two time periods using a one-dimensional bulk model that allows for the  
440 separation of changes in terms of seasonal freshwater input and vertical mixing (Fig. 2; Section  
441 3). While upper-ocean dynamics are significantly influenced by spatial and year-to-year variability  
442 (Fig. 1; e.g., Yamamoto-Kawai et al. 2009; Peralta-Ferriz and Woodgate 2015; Perovich and  
443 Richter-Menge 2015; Proshutinsky et al. 2019; Cole and Stadler 2019), we find that differences

444 between the ITP and AIDJEX datasets yield results that are consistent with decadal trends in the  
445 Canada Basin reported by previous studies (Peralta-Ferriz and Woodgate (2015); Section 4a).

446 By examining the relationships between bulk estimates of the freshwater input ( $h_{melt}$ ), vertical  
447 mixing ( $D$ ), and stratification ( $\delta S_{surf}$ ,  $S_z$ ), we found that two separate factors have a similar impact  
448 on creating the stronger stratification in 2006-2012 when compared with 1975: larger freshwater  
449 input and less vertical mixing (Figs. 8, 9, 10). These results stem from the finding that profiles  
450 with the same freshwater input are often associated with less vertical mixing and a more stratified  
451 upper-ocean in 2006-2012 relative to 1975, particularly in June–July (Fig. 8). In these cases, the  
452 stronger stratification in 2006-2012 relative to 1975 appears to be unrelated to seasonal freshwater  
453 surface fluxes. These results indicate that ice-ocean dynamics, rather than freshwater input alone,  
454 play a crucial role in explaining decadal changes to the seasonal halocline in the Canada Basin.

455 *Acknowledgments.* The AIDJEX data used in this study can be found at [http://lwbin-](http://lwbin-datahub.ad.umanitoba.ca/dataset/aidjex)  
456 [datahub.ad.umanitoba.ca/dataset/aidjex](http://lwbin-datahub.ad.umanitoba.ca/dataset/aidjex). The Ice-Tethered Profiler data were collected and made  
457 available by the Ice-Tethered Profiler Program based at the Woods Hole Oceanographic Institution  
458 (<http://www.whoi.edu/itp>). All sea ice concentration data created or used during this study are  
459 openly available from the NASA National Snow and Ice Data Center Distributed Active Archive  
460 Center at <https://doi.org/10.5067/8GQ8LZQVL0VL> as cited in (Cavalieri et al. 1996).

461 ER was supported by the National Sciences and Engineering Research Council of Canada  
462 (NSERC) PDF award, the Chateaubriand Fellowship of the Office for Science and Technology  
463 of the Embassy of France in the United States, and the US National Science Foundation (NSF)  
464 Graduate Research Fellowship. ER and JS were supported by the NSERC Canada-150 Chair.  
465 STG was supported by the US NSF (Awards PLR-1425989 and OPP-1936222) and by the US De-  
466 partment of Energy (DOE) (Award DE-SC0020073). This work is a contribution to the NSERC

467 - Discovery Grant and the NSF Office of Polar Program grant # 1504023 awarded to LBT. RG  
468 was supported by the NSERC Canada Discovery Grant program. RF acknowledges funding from  
469 NSERC Canada through a CGS-D award and the US DOE (Grant DE-SC001940). The authors  
470 thank Sheldon Bacon, Ursula Schauer, and one anonymous reviewer for helpful comments and  
471 suggestions.

## 472 **References**

473 Barthélemy, A., T. Fichefet, H. Goosse, and G. Madec, 2015: Modeling the interplay between sea  
474 ice formation and the oceanic mixed layer: Limitations of simple brine rejection parameteriza-  
475 tions. *Ocean Modelling*, **86**, 141–152, doi:10.1016/j.ocemod.2014.12.009.

476 Brown, K. A., J. M. Holding, and E. C. Carmack, 2020: Understanding regional and seasonal  
477 variability is key to gaining a pan-Arctic Perspective on Arctic Ocean freshening. *Frontiers*  
478 *Mar. Sci.*, **7**, 606, doi:10.3389/fmars.2020.00606.

479 Carmack, E., and Coauthors, 2015: Towards quantifying the increasing role of oceanic heat in  
480 sea ice loss in the new Arctic. *Bulletin of the American Meteorological Society*, doi:10.1175/  
481 BAMS-D-13-00177.1.

482 Carmack, E. C., and Coauthors, 2016: Freshwater and its role in the Arctic Marine System:  
483 Sources, disposition, storage, export, and physical and biogeochemical consequences in the  
484 Arctic and global oceans. *Journal of Geophysical Research: Biogeosciences*, **121**, 675–717,  
485 doi:10.1002/2015JG003140.

486 Cavalieri, D., C. L. Parkinson, P. Gloersen, and H. J. Zwally, 1996: Sea Ice Concentrations from  
487 SMMR and DMSP SSM/I-SSMIS Passive Microwave Data, Version1. *Natl. Snow and Ice Data*  
488 *Cent., Boulder, Colo.*, (Updated 2015.) <https://nsidc.org/data/nsidc-0051>.



489 Cole, S. T., and J. Stadler, 2019: Deepening of the winter mixed layer in the Canada Basin, Arctic  
490 Ocean over 2006-2017. *Journal of Geophysical Research: Oceans*, doi:10.1029/2019JC014940.

491 Davis, P. E. D., C. Lique, H. L. Johnson, and J. D. Guthrie, 2016: Competing effects of ele-  
492 vated vertical mixing and increased freshwater input on the stratification and sea ice cover in a  
493 changing Arctic Ocean. *Journal of Physical Oceanography*, doi:10.1175/JPO-D-15-0174.1.

494 Gallaher, S., T. Stanton, W. Shaw, S.-H. Kang, J.-H. Kim, and K.-H. Cho, 2017: Field observations  
495 and results of a 1-D boundary layer model for developing near-surface temperature maxima in  
496 the Western Arctic. *Elementa*, **5**, 1–21, doi:10.1525/elementa.195.

497 Gallaher, S. G., T. P. Stanton, W. J. Shaw, S. T. Cole, J. M. Toole, J. P. Wilkinson, T. Maksym, and  
498 B. Hwang, 2016: Evolution of a Canada Basin ice-ocean boundary layer and mixed layer across  
499 a developing thermodynamically forced marginal ice zone. *Journal of Geophysical Research:*  
500 *Oceans*, **121**, 6223–6250, doi:10.1002/2016JC011778.

501 Galley, R. J., B. G. T. Else, S. J. Prinsberg, D. Babb, and D. G. Barber, 2013: Sea ice con-  
502 centration, extent, age, motion and thickness in regions of proposed offshore oil and gas de-  
503 velopment near the Mackenzie Delta – Canadian Beaufort Sea. *Arctic*, **66(1)**, 105–116, doi:  
504 10.1029/2018MS001291.

505 Gudkovich, Z. M., 1961: Relation of the ice drift in the Arctic Basin to ice conditions in Soviet  
506 Arctic seas (in Russian). *Tr. Okeanogr. Kom. Akad.*, 11,14–21.

507 Hakkinen, S., A. Proshutinsky, and I. Ashok, 2008: Sea ice drift in the Arctic since the 1950s.  
508 *Geophysical Research Letters*, **35**, L19 704, doi:10.1029/2008GL034791.

509 Holloway, G., and Coauthors, 2007: Water properties and circulation in Arctic Ocean models.  
510 *Journal of Geophysical Research: Oceans*, **112 (4)**, 1–18, doi:10.1029/2006JC003642.

- 511 Hunkins, K., and J. A. Whitehead, 1992: Laboratory simulation of exchange through Fram Strait.  
512 *Journal of Geophysical Research*, **97(C7)**, 11,299–11,322, doi:10.1029/92JC00735.
- 513 Hutchings, J. K., and M. K. Faber, 2018: Sea-ice morphology change in the Canada Basin sum-  
514 mer: 2006–2015 ship observations compared to observations from the 1960s to the early 1990s.  
515 *Frontiers in Earth Science*, **6**, 2006–2015, doi:10.3389/feart.2018.00123.
- 516 Ilicak, M., and Coauthors, 2016: An assessment of the Arctic Ocean in a suite of interannual  
517 CORE-II simulations. Part III: Hydrography and fluxes. *Ocean Modelling*, **100**, 141–161.
- 518 Jackson, J. M., E. C. Carmack, F. A. McLaughlin, S. E. Allen, and R. G. Ingram, 2010:  
519 Identification, characterization, and change of the near-surface temperature maximum in the  
520 Canada Basin, 1993–2008. *Journal of Geophysical Research: Oceans*, **115**, 1–16, doi:10.1029/  
521 2009JC005265.
- 522 Jin, M., J. Hutchings, Y. Kawaguchi, and T. Kikuchi, 2012: Ocean mixing with lead-dependent  
523 subgrid scale brine rejection parameterization in a climate model. *Journal of Ocean University  
524 of China*, **11 (4)**, 473–480, doi:10.1007/s11802-012-2094-4.
- 525 Kern, S., A. Rösel, L. Toudal Pedersen, N. Ivanova, R. Saldo, and R. Tage Tonboe, 2016: The  
526 impact of melt ponds on summertime microwave brightness temperatures and sea-ice concen-  
527 trations. *Cryosphere*, **10**, 2217–2239, doi:10.5194/tc-10-2217-2016.
- 528 Kraus, E. B., and J. S. Turner, 1967: A one-dimensional model of the seasonal thermocline II. The  
529 general theory and its consequences. *Tellus*, **19 (1)**, 98–106, doi:10.3402/tellusa.v19i1.9753.
- 530 Krishfield, R., J. Toole, A. Proshutinsky, and M. L. Timmermans, 2008: Automated ice-tethered  
531 profilers for seawater observations under pack ice in all seasons. *Journal of Atmospheric and  
532 Oceanic Technology*, **25 (11)**, 2091–2105, doi:10.1175/2008JTECHO587.1.

533 Kwok, R., 2018: Arctic sea ice thickness, volume, and multiyear ice coverage: Losses and coupled  
534 variability (1958-2018). *Environmental Research Letters*, **13**, doi:10.1088/1748-9326/aae3ec.

535 Kwok, R., and D. A. Rothrock, 2009: Decline in Arctic sea ice thickness from submarine and ICE-  
536 Sat records: 1958-2008. *Geophysical Research Letters*, **36**, 1–5, doi:10.1029/2009GL039035.

537 Kwok, R., G. Spreen, and S. Pang, 2013: Arctic sea ice circulation and drift speed: Decadal  
538 trends and ocean currents. *Journal of Geophysical Research: Oceans*, **118** (5), 2408–2425, doi:  
539 10.1002/jgrc.20191.

540 Lemke, P., 1987: A coupled one-dimensional sea ice-ocean model. *Journal of Geophysical Re-  
541 search*, **92**, 164–172.

542 Lemke, P., and T. O. Manley, 1984: The seasonal variation of the mixed layer and the  
543 pycnocline under polar sea ice. *Journal of Geophysical Research*, **89**, 6494, doi:10.1029/  
544 JC089iC04p06494.

545 Lique, C., 2015: Ocean science: Arctic sea ice heated from below. *Nature Geoscience*, 1–2, doi:  
546 10.1038/ngeo2357.

547 Macdonald, R. W., E. C. Carmack, F. A. McLaughlin, K. K. Falkner, and J. H. Swift, 1999:  
548 Connections among ice, runoff and atmospheric forcing in the Beaufort Gyre. *Geophysical  
549 Research Letters*, **26** (15), 2223–2226, doi:10.1029/1999GL900508.

550 Martin, T., M. Steele, and J. Zhang, 2014: Seasonality and long-term trend of Arctic Ocean surface  
551 stress in a model. *Journal of Geophysical Research: Oceans*, **119**, 1723–1738, doi:10.1002/  
552 2013JC009425.

553 Martin, T., M. Tsamados, D. Schroeder, and D. L. Feltham, 2016: The impact of variable sea ice  
554 roughness on changes in Arctic Ocean surface stress: A model study. *Journal of Geophysical*  
555 *Research: Oceans*, **121**, 1931–1952, doi:10.1002/2015JC011186.

556 Martinson, D. G., 1990: Evolution of the Southern Ocean winter mixed layer and sea ice: Open  
557 ocean deepwater formation and ventilation. *Journal of Geophysical Research*, **95 (C7)**, 11 641,  
558 doi:10.1029/JC095iC07p11641.

559 Martinson, D. G., and R. Iannuzzi, 1998: Antarctic ocean-ice interactions: Implication from ocean  
560 bulk property distributions in the Weddell Gyre. *Antarctic sea ice: Physical processes, interac-*  
561 *tions and variability, Antarctic Research Series*, **74**, 243–271, doi:10.1029/AR074p0243.

562 Maykut, G. A., and M. G. McPhee, 1995: Solar heating of the Arctic mixed layer. *Journal of*  
563 *Geophysical Research*, **100**, 24 691, doi:10.1029/95JC02554.

564 McLaughlin, F., E. Carmack, A. Proshutinsky, R. Krishfield, C. Guay, M. Yamamoto-Kawai,  
565 J. Jackson, and B. Williams, 2011: The rapid response of the Canada Basin to climate forc-  
566 ing. *Oceanography*, **24**, 136–145, doi:10.5670/oceanog.2011.66.

567 McLaughlin, F. A., and E. C. Carmack, 2010: Deepening of the nutricline and chlorophyll max-  
568 imum in the Canada Basin interior, 2003-2009. *Geophysical Research Letters*, **37 (24)**, 1–5,  
569 doi:10.1029/2010GL045459.

570 McPhee, M. G., 2012: Advances in understanding ice – ocean stress during and since AIDJEX.  
571 *Cold Regions Science and Technology*, **76-77**, 24–36, doi:10.1016/j.coldregions.2011.05.001.

572 McPhee, M. G., and J. D. Smith, 1976: Measurements of the turbulent boundary layer under pack  
573 ice. *Journal of Physical Oceanography*, **6**, 696–711, doi:10.1175/1520-0485(1976)006<0696:  
574 MOTTBL>2.0.CO;2.

575 McPhee, M. G., T. P. Stanton, J. H. Morison, and D. G. Martinson, 1998: Freshening of the upper  
576 ocean in the Arctic: Is perennial sea ice disappearing? *Geophysical Research Letters*, **25**, 1729,  
577 doi:10.1029/98GL00933.

578 Meneghello, G., J. Marshall, C. Lique, P. E. Isachsen, E. Doddridge, J. M. Campin, H. Regan,  
579 and C. Talandier, 2021: Genesis and decay of mesoscale baroclinic eddies in the seasonally  
580 ice-covered interior arctic ocean. *Journal of Physical Oceanography*, **51** (1), 115–129, doi:  
581 10.1175/JPO-D-20-0054.1.

582 Meneghello, G., J. Marshall, M. L. Timmermans, and J. Scott, 2018: Observations of seasonal up-  
583 welling and downwelling in the Beaufort Sea mediated by sea ice. *Journal of Physical Oceanog-*  
584 *raphy*, **48** (4), 795–805, doi:10.1175/JPO-D-17-0188.1.

585 Morison, J., and J. D. Smith, 1981: Seasonal variations in the upper Arctic Ocean as observed at  
586 T-3. *Geophysical Research Letters*, **8**, 753–756, doi:10.1029/GL008i007p00753.

587 Newton, B., L. B. Tremblay, M. A. Cane, and P. Schlosser, 2006: A simple model of the Arc-  
588 tic Ocean response to annular atmospheric modes. *Journal of Geophysical Research: Oceans*,  
589 **111** (9), 1–13, doi:10.1029/2004JC002622.

590 Nguyen, A. T., D. Menemenlis, and R. Kwok, 2009: Improved modeling of the arctic halo-  
591 cline with a subgrid-scale brine rejection parameterization. *Journal of Geophysical Research:*  
592 *Oceans*, **114** (11), 1–12, doi:10.1029/2008JC005121.

593 Nummelin, A., C. Li, and L. H. Smedsrud, 2015: Response of Arctic Ocean stratification to  
594 changing river runoff in a column model. *Journal of Geophysical Research C: Oceans*, **120** (4),  
595 2655–2675, doi:10.1002/2014JC010571.

596 Parkinson, C. L., J. C. Comiso, H. J. Zwally, W. N. Meier, and J. Stroeve, 2004: Nimbus-5 ESMR  
597 Polar Gridded Sea Ice Concentrations, Version 1. *Natl. Snow and Ice Data Cent., Boulder, Colo.,*  
598 (Updated 2019.) <https://nsidc.org/data/nsidc-0009>.

599 Peralta-Ferriz, C., and R. A. Woodgate, 2015: Seasonal and interannual variability of pan-Arctic  
600 surface mixed layer properties from 1979 to 2012 from hydrographic data, and the dominance of  
601 stratification for multiyear mixed layer depth shoaling. *Progress in Oceanography*, **134**, 19–53,  
602 doi:10.1016/j.pocean.2014.12.005.

603 Perovich, D., 2011: The Changing Arctic Sea Ice Cover. *Oceanography*, **24 (3)**, 162–173, doi:  
604 doi.org/10.5670/oceanog.2011.68.

605 Perovich, D. K., and J. A. Richter-Menge, 2015: Regional variability in sea ice melt in a changing  
606 Arctic. *Phil.Trans.R.Soc.A 373*., **373**, doi:10.1098.

607 Petty, A. a., D. L. Feltham, and P. R. Holland, 2013: Impact of atmospheric forcing on Antarctic  
608 continental shelf water masses. *Journal of Physical Oceanography*, **43 (5)**, 920–940, doi:10.  
609 1175/JPO-D-12-0172.1.

610 Polyakov, I. V., and Coauthors, 2020: Borealization of the Arctic Ocean in response to anomalous  
611 advection From sub-Arctic seas. *Frontiers in Marine Science*, **7**, 1–81, doi:10.3389/fmars.2020.  
612 00491.

613 Proshutinsky, A., and Coauthors, 2009: Beaufort Gyre freshwater reservoir: State and variability  
614 from observations. *Journal of Geophysical Research*, **114**, doi:10.1029/2008JC005104.

615 Proshutinsky, A., and Coauthors, 2019: Analysis of the Beaufort Gyre freshwater content  
616 in 2003–2018. *Journal of Geophysical Research: Oceans*, **124**, 9658–9689, doi:10.1029/  
617 2019JC015281.

618 Rampal, P., J. Weiss, and D. Marsan, 2009: Positive trend in the mean speed and deformation  
619 rate of Arctic sea ice, 1979-2007. *Journal of Geophysical Research: Oceans*, **114** (5), 1–14,  
620 doi:10.1029/2008JC005066.

621 Randelhoff, A., I. Fer, and A. Sundfjord, 2017: Turbulent upper-ocean mixing affected by melt-  
622 water layers during Arctic summer. *Journal of Physical Oceanography*, **47** (4), 835–853, doi:  
623 10.1175/jpo-d-16-0200.1.

624 Reed, R. J., and B. A. Kunkel, 1960: The Arctic circulation in summer. *Journal of Meteorology*,  
625 **17**, 489–506, doi:10.1175/1520-0469(1960)017<0489:TACIS>2.0.CO;2.

626 Rosenblum, E., R. Fajber, J. C. Stroeve, S. T. Gille, L. B. Tremblay, and E. C. Carmack, 2021: Sur-  
627 face salinity under transitioning ice cover in the Canada Basin: Climate model biases linked to  
628 vertical distribution of fresh water. *Geophysical Research Letters*, doi:10.1029/2021GL094739.

629 Schauer, U., and M. Losch, 2019: Freshwater in the ocean is not a useful parameter in climate  
630 research. *Journal of Physical Oceanography*, **49** (9), 2309–2321, doi:10.1175/JPO-D-19-0102.  
631 1.

632 Schwejger, A., R. Lindsay, J. Zhang, M. Steele, and H. Stern, 2011: Uncertainty in modeled Arctic  
633 sea ice volume. *Journal of Geophysical Research*.

634 Sidorenko, D., and Coauthors, 2018: Influence of a Salt Plume Parameterization in a Coupled  
635 Climate Model. *Journal of Advances in Modeling Earth Systems*, **10** (9), 2357–2373, doi:10.  
636 1029/2018MS001291.

637 Spreen, G., R. Kwok, and D. Menemenlis, 2011: Trends in Arctic sea ice drift and role of wind  
638 forcing: 1992 - 2009. *Geophysical Research Letters*, **38**, L19 501, doi:10.1029/2008GL034791.

- 639 Steele, M., W. Ermold, and J. Zhang, 2011: Modeling the formation and fate of the near-surface  
640 temperature maximum in the Canadian Basin of the Arctic Ocean. *Journal of Geophysical Re-*  
641 *search*, **116**, C11 015, doi:10.1029/2010JC006803.
- 642 Stroeve, J., and D. Notz, 2018: Changing state of Arctic sea ice across all seasons. *Environmental*  
643 *Research Letters*, **13**, doi:10.1088/1748-9326/aade56.
- 644 Stroeve, J. C., T. Markus, L. Boisvert, J. Miller, and A. Barret, 2014: Changes in Arctic melt  
645 season and implications for sea ice loss. *Geophysical Research Letters*, **41**, 1216–1225, doi:  
646 10.1002/2013GL058951.
- 647 Timmermans, M., and J. Marshall, 2020: Understanding Arctic Ocean circulation: A review of  
648 ocean dynamics in a changing climate. *Journal of Geophysical Research: Oceans*, **125**, 1–35,  
649 doi:10.1029/2018jc014378.
- 650 Timmermans, M.-L., J. Toole, R. Krishfield, and P. Winsor, 2008: Ice-Tethered Profiler observa-  
651 tions of the double-diffusive staircase in the Canada Basin thermocline. *Journal of Geophys-*  
652 *ical Research*, **113**, C00A02, doi:10.1029/2008JC004829, URL [http://doi.wiley.com/10.1029/](http://doi.wiley.com/10.1029/2008JC004829)  
653 [2008JC004829](http://doi.wiley.com/10.1029/2008JC004829).
- 654 Timmermans, M. L., and P. Winsor, 2013: Scales of horizontal density structure in the Chukchi  
655 Sea surface layer. *Continental Shelf Research*, **52**, 39–45, doi:10.1016/j.csr.2012.10.015.
- 656 Tivy, A., S. E. Howell, B. Alt, S. McCourt, R. Chagnon, G. Crocker, T. Carrieres, and J. J. Yackel,  
657 2011: Trends and variability in summer sea ice cover in the Canadian Arctic based on the Cana-  
658 dian Ice Service Digital Archive, 1960-2008 and 1968-2008. *Journal of Geophysical Research:*  
659 *Oceans*, **116**, doi:10.1029/2009JC005855.



660 Toole, J. M., M. L. Timmermans, D. K. Perovich, R. A. Krishfield, A. Proshutinsky, and J. A.  
661 Richter-Menge, 2010: Influences of the ocean surface mixed layer and thermohaline stratifica-  
662 tion on Arctic Sea ice in the central Canada Basin. *Journal of Geophysical Research: Oceans*,  
663 **115**, 1–14, doi:10.1029/2009JC005660.

664 Tsamados, M., D. Feltham, A. Petty, D. Schroder, and D. Flocco, 2015: Processes controlling  
665 surface, bottom and lateral melt of Arctic sea ice in a state of the art sea ice model . *Philosophical*  
666 *Transactions of the Royal Society A*, **17**, 10 302, doi:10.1098/rsta.2014.0167.

667 Tsamados, M., D. L. Feltham, D. Schroeder, D. Flocco, S. L. Farrell, N. Kurtz, S. W. Laxon, and  
668 S. Bacon, 2014: Impact of variable atmospheric and oceanic form drag on simulations of arctic  
669 sea ice. *Journal of Physical Oceanography*, **44**, 1329–1353, doi:10.1175/JPO-D-13-0215.1.

670 Turner, J., 1967: A one-dimensional model of the seasonal thermocline I. A laboratory experiment  
671 and its interpretation. *Tellus*, **19** (1), 88–97, URL [http://onlinelibrary.wiley.com/doi/10.1111/j.](http://onlinelibrary.wiley.com/doi/10.1111/j.2153-3490.1967.tb01461.x/abstract)  
672 [2153-3490.1967.tb01461.x/abstract](http://onlinelibrary.wiley.com/doi/10.1111/j.2153-3490.1967.tb01461.x/abstract).

673 Untersteiner, N., A. S. Thorndike, D. A. Rothrock, and K. L. Hunkins, 2007: AIDJEX revisited:  
674 A look back at the U.S.-Canadian Arctic Ice Dynamics Joint Experiment 1970-78. *Arctic*, **60**,  
675 327–336, doi:10.14430/arctic233.

676 Wadhams, P., 2012: New predictions of extreme keel depths and scour frequencies for the Beaufort  
677 Sea using ice thickness statistics. *Cold Regions Science and Technology*, **76-77**, 77–82, doi:  
678 10.1016/j.coldregions.2011.12.002.

679 Yamamoto-Kawai, M., F. A. McLaughlin, E. C. Carmack, S. Nishino, K. Shimada, and N. Kurita,  
680 2009: Surface freshening of the Canada Basin, 2003-2007: River runoff versus sea ice meltwa-  
681 ter. *Journal of Geophysical Research: Oceans*, **114**, 2003–2007, doi:10.1029/2008JC005000.

682 Zhang, J., and M. Steele, 2007: Effect of vertical mixing on the Atlantic Water layer circulation  
683 in the Arctic Ocean. *Journal of Geophysical Research: Oceans*, **112** (4), 1–9, doi:10.1029/  
684 2006JC003732.

685 **LIST OF TABLES**

686 **Table 1.** List of AIDJEX ice camps and ITPs used in the study. . . . . 35

687 **Table 2.** List of constants and variable names. . . . . 36

TABLE 1. List of AIDJEX ice camps and ITPs used in the study.

Ice Camp	Time Period Used
Blue Fox	May 10, 1975 - Sept. 31, 1975
Caribou	May 14, 1975 - Sept. 31, 1975
Snowbird	May 16, 1975 - Sept. 31, 1975
Big Bear	May 1, 1975 - Sept. 31, 1975
ITP	Time Period Used
1	May 1, 2006 - Sept. 31, 2006
3	May 1, 2006 - Sept. 10, 2006
4	May 1, 2007 - Aug. 17, 2007
5	May 1, 2007 - Aug. 2, 2007
6	May 1, 2007 - Sept. 31, 2007
8	May 1, 2008 - Sept. 31, 2008
11	May 1, 2009 - July 20, 2009
13	May 1, 2008 - Aug. 8, 2008
18	May 1, 2008 - Sept. 31, 2008
33	May 1, 2010 - Sept. 31, 2010
41	May 1, 2011 - Sept. 31, 2011
41	May 1, 2012 - Sept. 31, 2012
53	May 1, 2012 - Aug. 5, 2012

TABLE 2. List of constants and variable names.

Name	Description	Value/ Equation
$Z_{ice}$	ice-ocean interface	3 m
$\beta$	haline contraction coefficient	$0.81 \text{ kg}^2/\text{m}^3/\text{g}$
$\rho_{ice}$	sea ice density	$900 \text{ kg}/\text{m}^3$
$S_{ice}$	sea ice salinity	5 g/kg
$\delta S_{surf}$	seasonal surface freshening	eq. 15
$S_z$	stratification	eqs. 6,12
$S_{z,bulk}$	as in $S_z$ but for 2-layer system	eq.12
$h_{melt}$	freshwater input in terms of ice melt	eq. 3
$\Phi$	measure of freshwater input	eq. 4
$Z_{fw}$	penetration depth of freshwater input	eq. 3
$D$	equivalent mixed-layer depth	eq. 10

688 **LIST OF FIGURES**

689 **Fig. 1.** Map of Canada Basin showing September sea ice concentration and location of ocean obser-  
690 vations. (Left) September 1975 mean sea ice concentration and location of measurements  
691 from AIDJEX sea ice camps (blue dots) and (right) 2006-2012 September-mean sea ice  
692 concentration and location of ITP observations (red dots). Region indicated by dashed-lines  
693 shows the Canada Basin, which we define as the region bounded by 72°N, 80°N, 130°W,  
694 and 155°W. Solid lines indicate bathymetric contours at 1000 m, 2000 m, and 3000 m. The  
695 regional map of September 1975 sea ice concentrations are provided by Nimbus-5 ESMR  
696 Polar Gridded Sea Ice Concentrations, Version 1 (Parkinson et al. 2004) . . . . . 39

697 **Fig. 2.** Schematic of one-dimension ice-ocean model, showing an illustration of the salinity profile  
698 resulting from ice melt that is concentrated close to the surface (left) and an example where  
699 a similar amount of ice melt is mixed over a larger depth range (right).  $L$  is the depth of the  
700 ocean.  $D$ ,  $Z_{ice}$ , and  $Z_{fw}$  are negative values that indicate depths.  $S_0$  and  $\delta S_{surf}$  indicate the  
701 initial salinity and surface freshening, respectively. Area covered by gray shading is equal  
702 to  $\Phi$  and linearly related to the equivalent sea ice melt ( $h_{melt}$ ). Vertical and horizontal blue  
703 dashed lines indicate  $D$  and  $\delta S_{surf}$ , respectively. Grey arrows represent the vertical extent  
704 of sea-ice meltwater. . . . . 40

705 **Fig. 3.** 10-day mean profiles during (a) May-July and (b) August-September in 1975 (blue) and  
706 2006-2012 (red). Solid black lines indicate 10-day mean profiles from (a) the beginning  
707 of May and (b) the end of September. Dashed lines indicate common 10-day mean profile  
708 that marks the end of July and the beginning of August, (July 30 - August 8) and are the  
709 same in panels a and b. Note that in May, when the freshwater input from sea ice melt is  
710 small, changes to the average near-surface salinity are small compared to the spatial and  
711 inter-annual variability (Fig. S1). . . . . 41

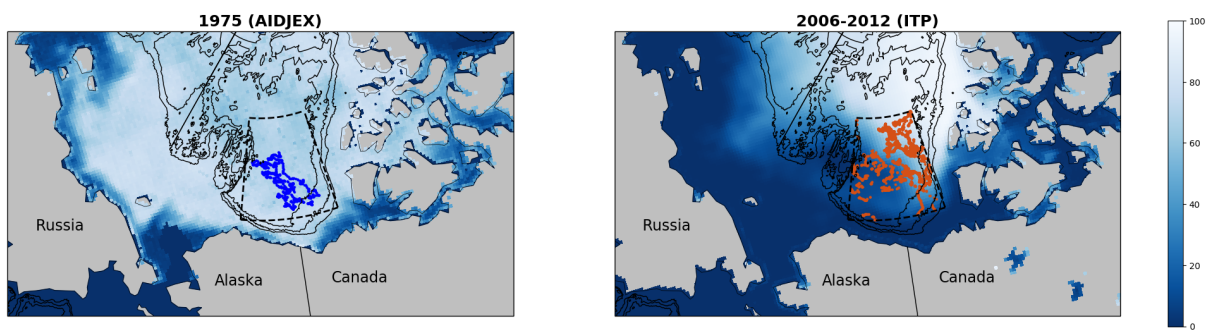
712 **Fig. 4.** Observed salinity profiles using data from (left) AIDJEX Big Bear ice camp in 1975 and  
713 (right) ITP #4 in 2007 to illustrate the methods used to estimate metrics derived in Section  
714 3. (a-b) All observed salinity profiles measured during the month of May (gray lines) and  
715 July (blue lines), with July 25th highlighted in dark blue ( $S(z)$ ). (c-d) Black line indicates  
716 May-average surface salinity ( $S_0$ ), area covered by gray shading is the same as  $\Phi$  associated  
717 with the observed July 25 profile. The associated 2-layer salinity profile (red dashed lines,  
718  $S_{bulk}(z)$ ), which give the surface freshening  $\delta S_{surf}$  and equivalent mixed-layer depth  $D$ , is  
719 shown in red. Blue lines are the same in panels (a,c) and (b,d). . . . . 42

720 **Fig. 5.** (a) Sea ice concentration and (b-c) estimated freshwater input in terms of cumulative sea ice  
721 thickness changes ( $h_{melt}$ ) in 1975 (blue), 2006-2012 (red). PIOMAS data provide a clima-  
722 tological monthly effective sea ice thickness change relative to May of each year between  
723 1979-2018 (black). Blue and red lines indicate 5-day mean, black lines indicate monthly  
724 mean, and shadings indicate one standard deviation. . . . . 43

725 **Fig. 6.** Validation of the 2-layer approximation of the salinity profile by comparing the stratification  
726 (left;  $S_z$ ; eq. 6) to the associated 2-layer estimate (center; eq. 12), and their difference (right)  
727 in 1975 (blue) and 2006-2012 (red).  $S_z$  is computed for each observed profile. Lines indicate  
728 5-day means and shading indicates one standard deviation (left, center panels) or standard  
729 error (right panels). . . . . 44

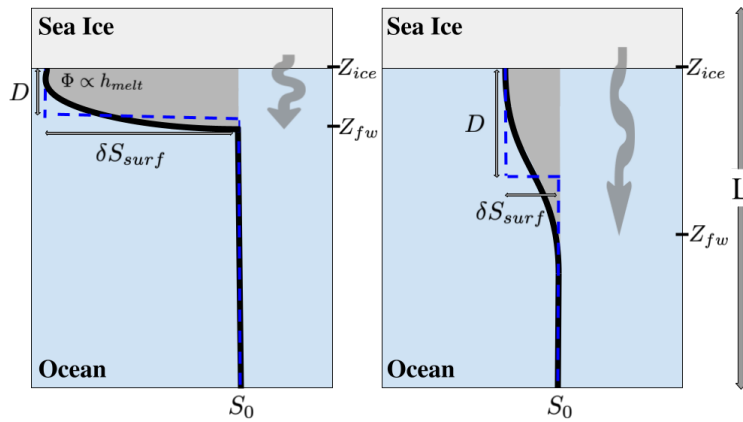
730 **Fig. 7.** (a) Surface freshening ( $\delta S_{surf}$ ) and (b) equivalent mixed-layer depth ( $D$ ) in 1975 (blue) and  
731 2006-2012 (red).  $\delta S_{surf}$  and  $D$  are computed for each observed profile. Lines indicate 5-day  
732 means and shading indicates one standard deviation. . . . . 45

733	<b>Fig. 8.</b> Relationships between equivalent sea ice melt ( $h_{melt}$ ) and (a,d) equivalent mixed-layer depth ( $D$ ), (b,e) surface freshening ( $\delta S_{surf}$ ), and (c,f) upper-ocean stratification ( $S_z$ ) using vertical salinity profiles in 1975 (blue) and 2006-2012 (red) during June-July (a-c) and August-September (d-f). Shadings indicate date of measurement. . . . .	46
734		
735		
736		
737	<b>Fig. 9.</b> Five-day average differences between 1975 and 2006-2012 using the difference between equivalent ice melt ( $\Delta h_{melt}$ ), the surface freshening ( $\Delta(\delta S_{surf})$ ), and stratification ( $\Delta S_z$ ) during the two time periods. Colors indicate month and lines indicate one standard error. . . . .	47
738		
739		
740		
741	<b>Fig. 10.</b> Five-day mean (a) equivalent ice melt ( $h_{melt}$ ), (b) surface freshening using the 2-layer estimate ( $\Delta S_{surf}$ ), and (c) stratification using the 2-layer estimate ( $S_z$ ) in 1975 (blue) and 2006-2012 (red). (b-c) Colors are associated with three terms that contribute to the difference between 1975 and 2006-2012 ( $\Delta(\delta S_{surf})$ , $\Delta S_z$ ). . . . .	48
742		
743		
744		

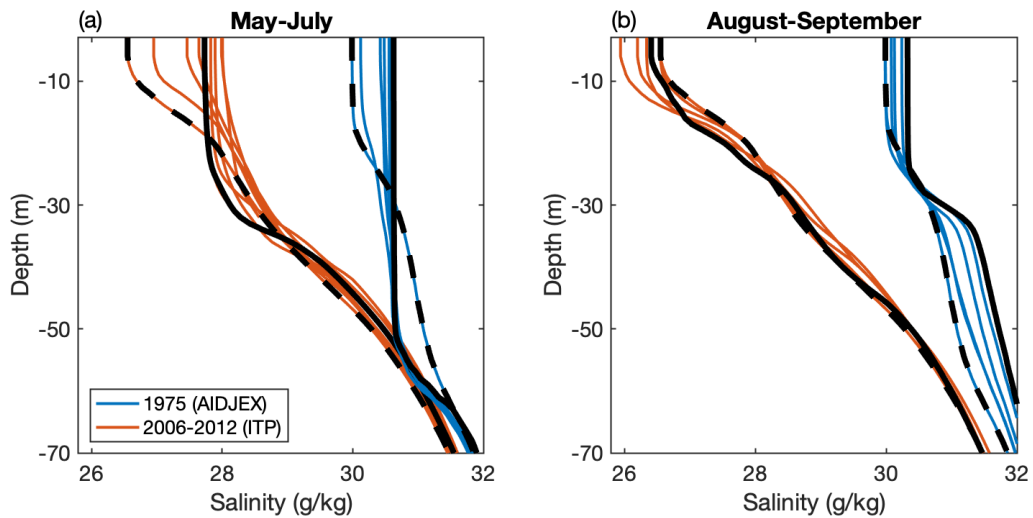


744 FIG. 1. Map of Canada Basin showing September sea ice concentration and location of ocean observations.  
 745 (Left) September 1975 mean sea ice concentration and location of measurements from AIDJEX sea ice camps  
 746 (blue dots) and (right) 2006-2012 September-mean sea ice concentration and location of ITP observations (red  
 747 dots). Region indicated by dashed-lines shows the Canada Basin, which we define as the region bounded by  
 748  $72^{\circ}\text{N}$ ,  $80^{\circ}\text{N}$ ,  $130^{\circ}\text{W}$ , and  $155^{\circ}\text{W}$ . Solid lines indicate bathymetric contours at 1000 m, 2000 m, and 3000 m. The  
 749 regional map of September 1975 sea ice concentrations are provided by Nimbus-5 ESMR Polar Gridded Sea Ice  
 750 Concentrations, Version 1 (Parkinson et al. 2004)

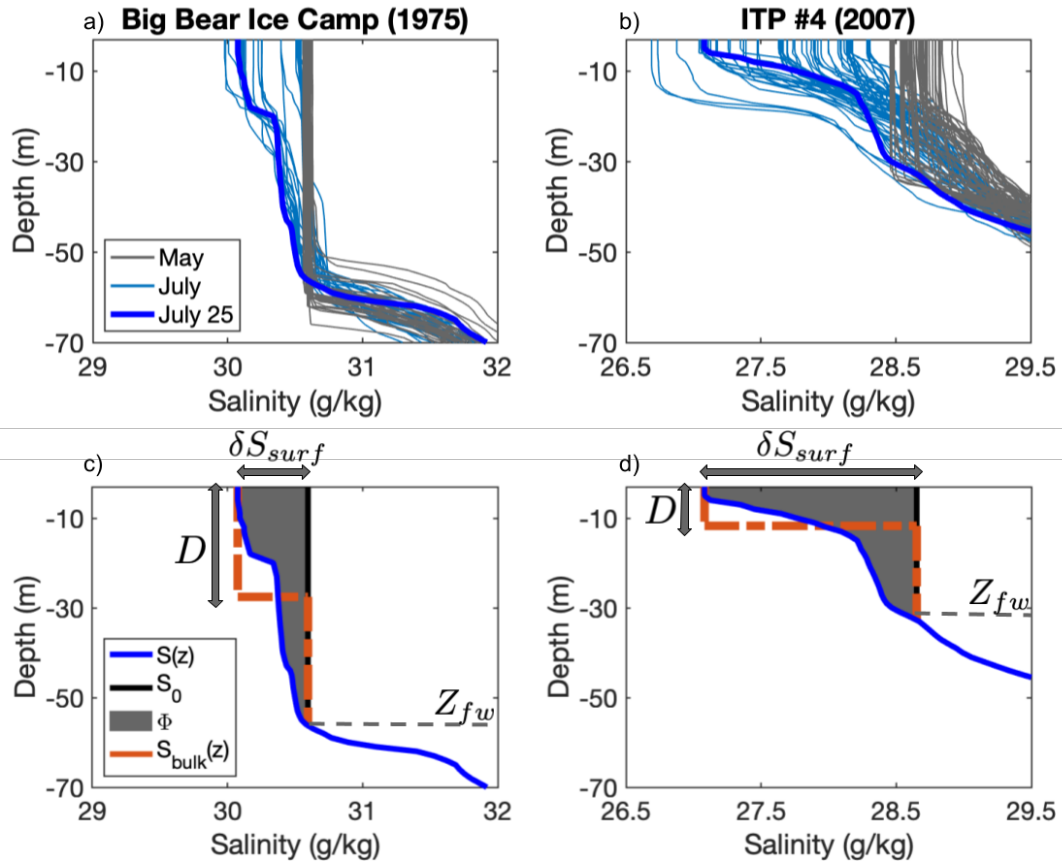




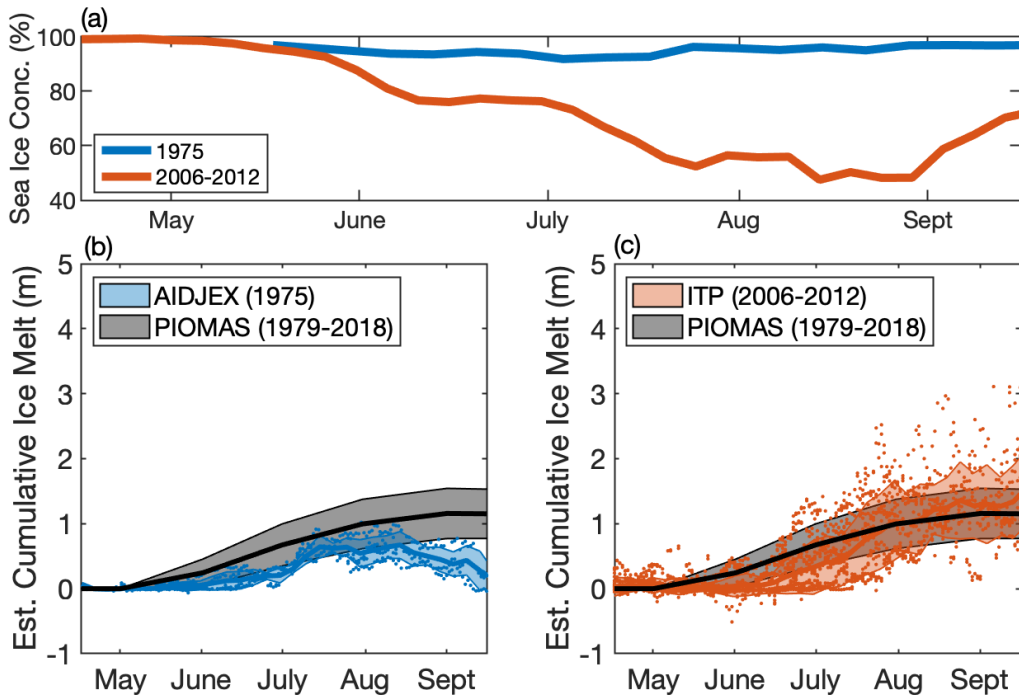
751 FIG. 2. Schematic of one-dimension ice-ocean model, showing an illustration of the salinity profile resulting  
 752 from ice melt that is concentrated close to the surface (left) and an example where a similar amount of ice melt  
 753 is mixed over a larger depth range (right).  $L$  is the depth of the ocean.  $D$ ,  $Z_{ice}$ , and  $Z_{fw}$  are negative values that  
 754 indicate depths.  $S_0$  and  $\delta S_{surf}$  indicate the initial salinity and surface freshening, respectively. Area covered by  
 755 gray shading is equal to  $\Phi$  and linearly related to the equivalent sea ice melt ( $h_{melt}$ ). Vertical and horizontal blue  
 756 dashed lines indicate  $D$  and  $\delta S_{surf}$ , respectively. Grey arrows represent the vertical extent of sea-ice meltwater.



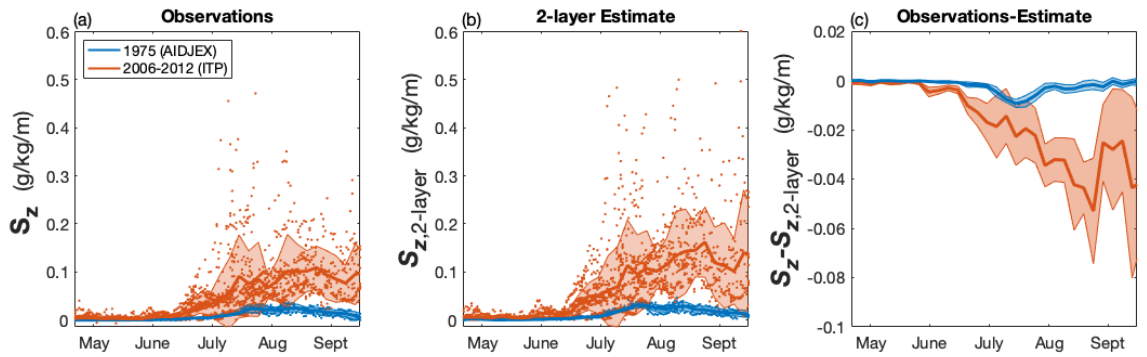
757 FIG. 3. 10-day mean profiles during (a) May-July and (b) August-September in 1975 (blue) and 2006-2012  
 758 (red). Solid black lines indicate 10-day mean profiles from (a) the beginning of May and (b) the end of Septem-  
 759 ber. Dashed lines indicate common 10-day mean profile that marks the end of July and the beginning of August,  
 760 (July 30 - August 8) and are the same in panels a and b. Note that in May, when the freshwater input from sea  
 761 ice melt is small, changes to the average near-surface salinity are small compared to the spatial and inter-annual  
 762 variability (Fig. S1).



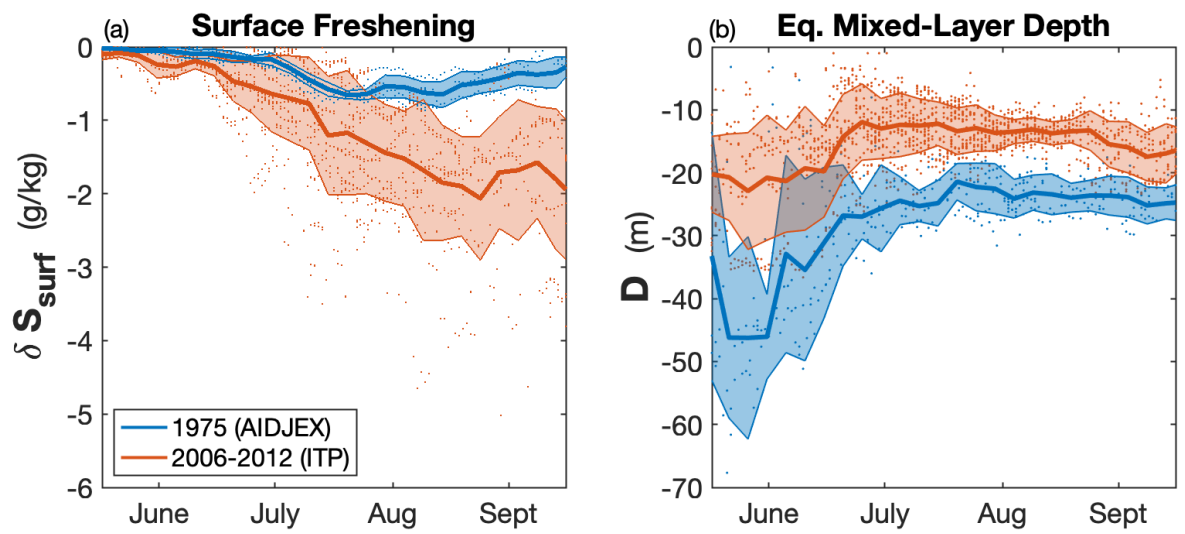
763 FIG. 4. Observed salinity profiles using data from (left) AIDJEX Big Bear ice camp in 1975 and (right) ITP  
 764 #4 in 2007 to illustrate the methods used to estimate metrics derived in Section 3. (a-b) All observed salinity  
 765 profiles measured during the month of May (gray lines) and July (blue lines), with July 25th highlighted in dark  
 766 blue ( $S(z)$ ). (c-d) Black line indicates May-average surface salinity ( $S_0$ ), area covered by gray shading is the  
 767 same as  $\Phi$  associated with the observed July 25 profile. The associated 2-layer salinity profile (red dashed lines,  
 768  $S_{bulk}(z)$ ), which give the surface freshening  $\delta S_{surf}$  and equivalent mixed-layer depth  $D$ , is shown in red. Blue  
 769 lines are the same in panels (a,c) and (b,d).



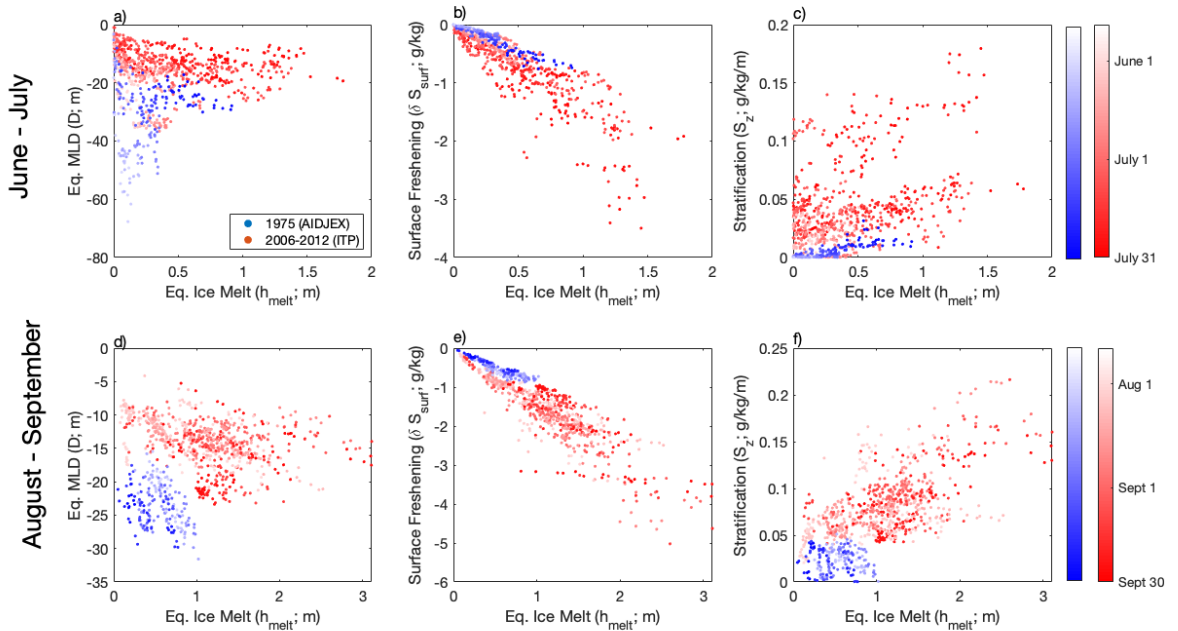
770 FIG. 5. (a) Sea ice concentration and (b-c) estimated freshwater input in terms of cumulative sea ice thickness  
 771 changes ( $h_{melt}$ ) in 1975 (blue), 2006-2012 (red). PIOMAS data provide a climatological monthly effective sea  
 772 ice thickness change relative to May of each year between 1979-2018 (black). Blue and red lines indicate 5-day  
 773 mean, black lines indicate monthly mean, and shadings indicate one standard deviation.



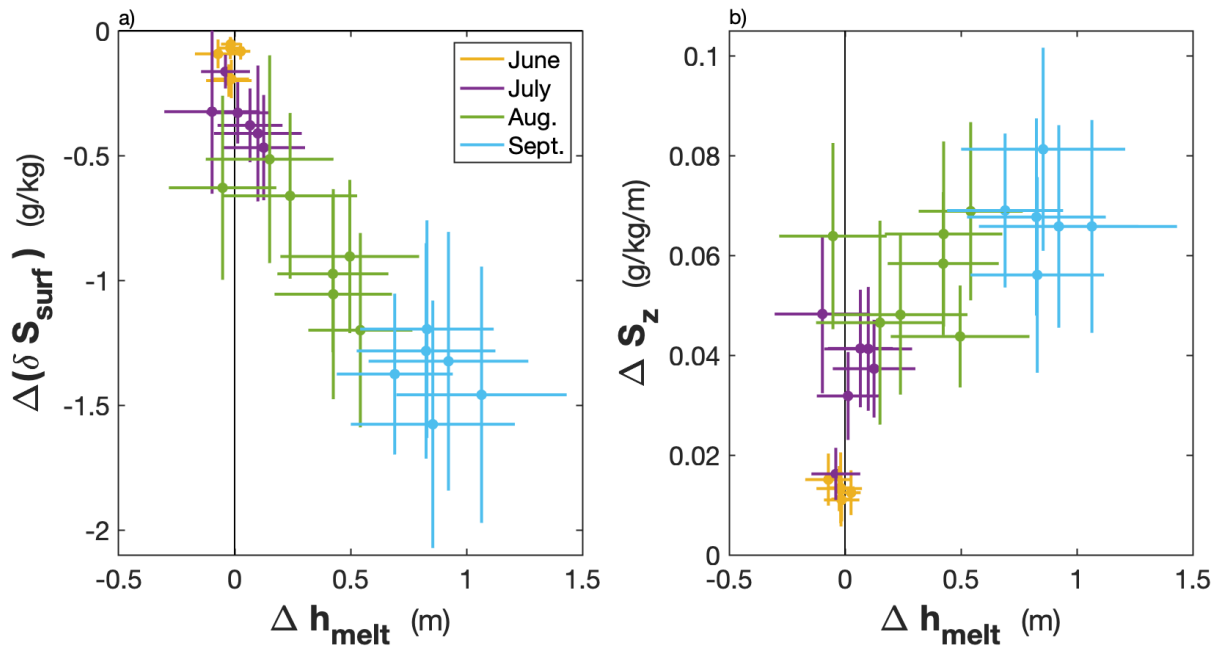
774 FIG. 6. Validation of the 2-layer approximation of the salinity profile by comparing the stratification (left;  
 775  $S_z$ ; eq. 6) to the associated 2-layer estimate (center; eq. 12), and their difference (right) in 1975 (blue) and  
 776 2006-2012 (red).  $S_z$  is computed for each observed profile. Lines indicate 5-day means and shading indicates  
 777 one standard deviation (left, center panels) or standard error (right panels).



778 FIG. 7. (a) Surface freshening ( $\delta S_{surf}$ ) and (b) equivalent mixed-layer depth ( $D$ ) in 1975 (blue) and 2006-2012  
 779 (red).  $\delta S_{surf}$  and  $D$  are computed for each observed profile. Lines indicate 5-day means and shading indicates  
 780 one standard deviation.

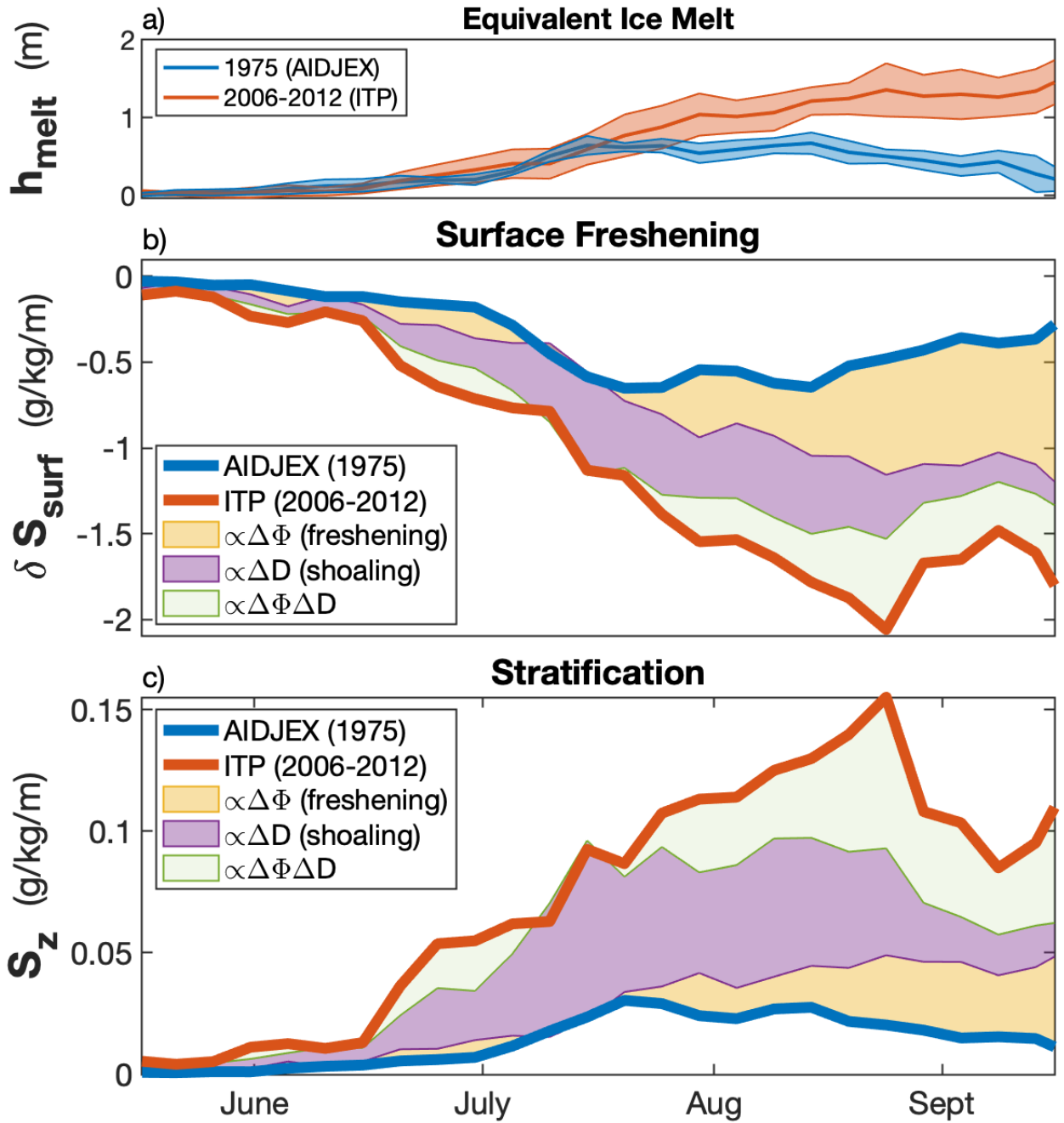


781 FIG. 8. Relationships between equivalent sea ice melt ( $h_{melt}$ ) and (a,d) equivalent mixed-layer depth ( $D$ ), (b,e)  
 782 surface freshening ( $\delta S_{surf}$ ), and (c,f) upper-ocean stratification ( $S_z$ ) using vertical salinity profiles in 1975 (blue)  
 783 and 2006-2012 (red) during June-July (a-c) and August-September (d-f). Shadings indicate date of measurement.



784 FIG. 9. Five-day average differences between 1975 and 2006-2012 using the difference between equivalent  
 785 ice melt ( $\Delta h_{melt}$ ), the surface freshening ( $\Delta(\delta S_{surf})$ ), and stratification ( $\Delta S_z$ ) during the two time periods. Colors  
 786 indicate month and lines indicate one standard error.





787 FIG. 10. Five-day mean (a) equivalent ice melt ( $h_{melt}$ ), (b) surface freshening using the 2-layer estimate  
 788 ( $\Delta S_{surf}$ ), and (c) stratification using the 2-layer estimate ( $S_z$ ) in 1975 (blue) and 2006-2012 (red). (b-c) Colors  
 789 are associated with three terms that contribute to the difference between 1975 and 2006-2012 ( $\Delta(\delta S_{surf})$ ,  $\Delta S_z$ ).